CAHEN, D., IBERS, J. A. & SHANNON, R. D. (1972). *Inorg. Chem.* **11**, 2311–2315.

CAHEN, D., IBERS, J. A. & WAGNER, J. B. (1974). *Inorg. Chem.* **13**, 1377–1388.

CRUICKSHANK, D. W. J. (1965). *Acta Cryst.* **19**, 153.

FUKUNDA, M. & ASAI, K. (1975). German patent 1,671,455.

GOODENOUGH, J. B. (1963). *Magnetism and the Chemical Bond.* New York: Interscience.

GOODENOUGH, J. B. (1971). *Prog. Solid State Chem.* **5**, 145–399.

HEWAT, A. W. (1973). UK Atomic Energy Authority Research Group Report RLL 73/897 (unpublished).

KOZIOL, K., SIEKERER, K.-H. & RUTHJEN, H. C. (1976). US patent 3,948,752.

LAZAREV, V. B. & SHAPLYGIN, I. S. (1978a). *Russ. J. Inorg. Chem.* **23**, 1610–1612.

LAZAREV, V. B. & SHAPLYGIN, I. S. (1978b). *Russ. J. Inorg. Chem.* **23**, 163–170.

LAZAREV, V. B. & SHAPLYGIN, I. S. (1978c). *Mater. Res. Bull.* **13**, 229–235.

MULLER, O. & ROY, R. (1968). *J. Less Common Met.* **16**, 129–146.

MÜLLNER, M., THIELE, G. & ZÖLLNER, C. (1978). *Z. Anorg. Allg. Chem.* **443**, 19–22.

RIETVELD, H. M. (1969a). Reactor Centrum Nederland Research Report RCN 104 (unpublished).

RIETVELD, H. M. (1969b). *J. Appl. Cryst.* **2**, 65–71.

ROBIN, M. & DAY, P. (1967). *Adv. Inorg. Chem. Radiochem.* **10**, 247–422.

SCHEER, J. J. (1956). PhD Thesis, Leyden.

SCHEER, J. J., VAN ARKEL, A. E. & HEYDING, R. D. (1955). *Can. J. Chem.* **33**, 683–686.

SCHWARTZ, K. B., PARISE, J. B., PREWITT, C. T. & SHANNON, R. D. (1981). In preparation.

SHANNON, R. D. (1969). *Solid State Commun.* **7**, 257.

SHANNON, R. D. (1976). *Acta Cryst.* A**32**, 751–767.

SUKHOTIN, A. M., GANKIN, E. A., KONDVASHOV, YU. D., OMEL'CHENKO, YU. D. & SHAL'MAN, B. YA. (1971). *Russ. J. Inorg. Chem.* **16**, 1690–1693.

THIELE, G., ZÖLLNER, G. & KOZIOL, K. (1973). GB patent 1,328,270.

THIELE, G., ZÖLLNER, G. & KOZIOL, K. (1976). US patent 4,042,484.

WASER, J. & McCLANAHAN, E. D. (1951). *J. Chem. Phys.* **19**, 413–416.

WILLIS, B. T. M. & PRYOR, A. W. (1975). *Thermal Vibrations in Crystallography.* Cambridge Univ. Press.

ZÖLLNER, C., THIELE, G. & MÜLLNER, M. (1978). *Z. Anorg. Allg. Chem.* **443**, 11–18.

ZÖLLNER, C., ZÖLLNER, G. & KOZIOL, K. (1976a). US patent 3,962,068.

ZÖLLNER, C., ZÖLLNER, G. & KOZIOL, K. (1976b). US patent 3,992,280.

Compounds with Perovskite-Type Slabs. V. A High-Temperature Modification of La₂Ti₂O₇

BY N. ISHIZAWA, F. MARUMO* AND S. IWAI

Research Laboratory of Engineering Materials, Tokyo Institute of Technology, Nagatsuta 4259, Midori, Yokohama 227, Japan ·

AND M. KIMURA AND T. KAWAMURA

Fundamental Research Laboratory, Nippon Electric Co. Ltd, Miyazaki 4-1-1, Takatsu-ku, Kawasaki, Japan

Abstract

La₂Ti₂O₇ with the monoclinic space group $P2_1$ transforms its structure into one with the orthorhombic space group $Cmc2_1$ at approximately 1053 K. The orthorhombic structure at 1173 ± 10 K with $a = 3.954$ (2), $b = 25.952$ (8) and $c = 5.607$ (2) Å and $Z = 4$ has been determined from three-dimensional X-ray diffraction data and refined to a conventional R value of 0.066 for 766 observed reflexions. The crystal is essentially isostructural with that of Sr₂Nb₂O₇, in which all atoms are on the mirror plane at $x = 0$ or 0.5 and the corner-shared BO_6 octahedra and A atoms with twelve coordination form perovskite-type slabs. The structural change between the orthorhombic and monoclinic modifications is characterized by displacements of La atoms taking place within the respective planes perpendicular to the a axis on which the relevant La atoms lie, and by rotations of TiO₆ octahedra around axes parallel to the b axis and running through the respective Ti atoms. No significant displacement of the Ti positions occurs. Half of the mirror planes in the orthorhombic modification are lost on the phase transition and the remaining half survive as local mirror

planes in the slabs, giving partial enhancement of the diffraction symmetry in the monoclinic low-temperature modification.

Introduction

Recently several ferroelectric $A_2B_2O_7$ compounds, including $Sr_2Ta_2O_7$, $Sr_2Nb_2O_7$, $La_2Ti_2O_7$, $Ca_2Nb_2O_7$ and $Nd_2Ti_2O_7$, were shown to form a structural family characterized by a perovskite-type slab. Various structural modifications of these compounds were analysed. Crystals of $La_2Ti_2O_7$ and $Ca_2Nb_2O_7$ have two modifications, one of which has the symmetry of $P2_1$ (Gasperin, 1975; Ishizawa, Marumo, Iwai, Kimura & Kawamura, 1980) and the other of $Pbn2_1$ (Scheunemann & Müller-Buschbaum, 1974, 1975). Both modifications have primitive unit cells and approximately the same a and c lengths (the first setting is employed for the monoclinic cell), while the cell volume of the monoclinic one is half that of the orthorhombic one. The orthorhombic structure can be obtained by stacking the unit cells of the monoclinic one along the b axis with the operation of an n glide plane parallel to (010) (Ishizawa et al., 1980). The structure of $Sr_2Ta_2O_7$ with the space group $Cmcm$ can be taken as the prototype of this family (Ishizawa, Marumo, Kawamura & Kimura, 1976). The structural changes between the $Cmcm$ and $Cmc2_1$ modifications were investigated for $Sr_2(Ta_{1-x}Nb_x)_2O_7$ ($x \simeq 0.12$) and $Sr_2Ta_2O_7$ (Ishizawa, Marumo & Iwai, 1981). Both modifications with the base-centred unit cells have approximately the same cell dimensions. The a lengths of these modifications are half of those with the symmetries $P2_1$ and $Pbn2_1$. The transitions between the base-centred and the primitive ones, however, were not known. Recently anomalies in the electromechanical coupling factors were found in $La_2Ti_2O_7$ at 993 and 1053 K (Kimura, 1977). The structural investigation of $La_2Ti_2O_7$ at elevated temperatures was, therefore, undertaken to afford information about respective $A_2B_2O_7$ compounds with perovskite-type slabs.

Experimental

Single crystals of $La_2Ti_2O_7$ were synthesized with the floating-zone technique on an image furnace (Nanamatsu, Kimura, Doi, Matsushita & Yamada, 1974). Crystals were transparent and colourless with micaceous cleavage parallel to (010). A Weissenberg camera equipped with a small platinum heater (Iwai, Tagai, Kato & Shimamune, 1971) was used to take the diffraction photographs of the specimen at various temperatures ranging from room temperature to approximately 1200 K. Crystals at temperatures below 993 K have partially enhanced diffraction symmetries.

If only the hkl reflexions with h even are taken into consideration, the symmetry is base-centred orthorhombic and identical to that of the prototype structure of this family. The reflexions with h odd are relatively weak and show monoclinic symmetry. The extinction rule is $0k0$ for k odd, and the space group is restricted to $P2_1$ from the ferroelectric property of the crystal. With increasing temperature, the reflexions with h odd become weaker and finally disappear at a temperature in the region 993 to 1053 K. The space group above 1053 K was confirmed to be $Cmc2_1$ on consideration of the fact that the crystal is ferroelectric below 1773 K (Nanamatsu et al., 1974). The relation between the $P2_1$ and $Cmc2_1$ unit cells is

$$\begin{pmatrix} a \\ b \\ c \end{pmatrix}_{P2_1} = \begin{pmatrix} 2 & 0 & 0 \\ -0.5 & 0.5 & 0 \\ 0 & 0 & 1 \end{pmatrix} \begin{pmatrix} a \\ b \\ c \end{pmatrix}_{Cmc2_1.}$$

With decreasing temperature in the region from 1053 to 993 K, the monoclinic reflexions again appear and become stronger. No detailed information was obtained about the structure in the region 993–1053 K. The reflexions with h even seemed scarcely affected by the phase transition. The existence of the $Pbn2_1$ modification was not recognized with the present $La_2Ti_2O_7$ crystals throughout the experiments.

Intensity collection and the determination of the cell dimensions at 1173 ± 10 K were carried out using a four-circle diffractometer (Rigaku) equipped with a high-temperature apparatus (Ishizawa, Miyata, Minato & Iwai, 1978). A crystal with dimensions 0.25 × 0.01 × 0.025 mm was mounted on the top of a silica-glass capillary. The Pt–Pt(13%Rh) thermocouple was placed in the capillary at a position 0.3 mm from the specimen. Mo $K\alpha$ radiation monochromated with pyrolitic graphite was used, with the crystal placed at the centre of a thin silica-glass ball (10 mm in diameter and approximately 0.1 mm thick) which was supplied with hot N_2 gas. Cell dimensions were determined from 10 2θ values of the reflexions in the range $0.2 < \sin \theta/\lambda < 0.5$ Å^{-1} with the least-squares procedure. Crystal data of $La_2Ti_2O_7$ are given in Table 1. Intensity data were collected in the range $\sin \theta/\lambda < 0.904$ Å^{-1}

Table 1. *Crystal data of* $La_2Ti_2O_7$

Crystal system	Room temperature		At 1173 K
	Monoclinic*	Orthorhombic†	Orthorhombic
Space group	$P2_1$	$Pbn2_1$	$Cmc2_1$
a (Å)	7.800 (3)	7.810	3.954 (2)
b (Å)	13.011 (4)	25.745	25.952 (8)
c (Å)	5.546 (2)	5.547	5.607 (2)
γ (°)	98.60 (2)		
Z	4	8	4

* Gasperin (1975).
† Scheunemann & Müller-Buschbaum (1975).

employing the ω–2θ scan technique with a scan speed of 2° min^{-1} in ω and the scan width determined from the formula $1.5° + 0.5°$ tan θ. Lorentz, polarization and absorption corrections were carried out assuming the crystal to be a rectangular parallelepiped. 766 independent reflexions were obtained whose $|F_o|$'s were larger than $3\sigma(|F_o|)$.

Since the Patterson maps calculated from the reflexion data were quite similar to those for $Sr_2Nb_2O_7$ (Ishizawa, Marumo, Kawamura & Kimura, 1975), the refinement of the structure was carried out with the full-matrix least-squares program *LINUS* (Coppens & Hamilton, 1970) using the positional parameters of $Sr_2Nb_2O_7$ for the starting values. Anisotropic temperature factors were used for the metal atoms and isotropic ones for the O atoms. Unit weight was allotted for all the reflexions. Atomic scattering factors and the real and imaginary dispersion terms were taken from *International Tables for X-ray Crystallography* (1974). The final R value was 0.066. Final positional

Table 2. *Positional and thermal parameters for* $La_2Ti_2O_7$ *at* 1173 K, *with their estimated standard deviations in parentheses*

	x	y	z	B_{eq}/B (Å^2)
La(1)	0	0.44609 (6)	0.75	2.18 (4)*
La(2)	0	0.29808 (8)	0.1757 (5)	3.05 (7)*
Ti(1)	0.5	0.4404 (1)	0.2452 (11)	1.55 (8)*
Ti(2)	0.5	0.3370 (1)	0.7095 (8)	1.58 (11)*
O(1)	0.5	0.5088 (9)	0.475 (5)	3.2 (5)
O(2)	0.5	0.4077 (8)	0.542 (4)	2.3 (3)
O(3)	0.5	0.2964 (8)	0.458 (5)	2.8 (4)
O(4)	0	0.4511 (8)	0.255 (7)	2.9 (3)
O(5)	0	0.3472 (7)	0.720 (5)	3.0 (4)
O(6)	0.5	0.3891 (10)	0.039 (6)	3.6 (5)
O(7)	0.5	0.2818 (8)	0.935 (4)	2.2 (3)

* $B_{eq} = 8\pi^2 (U_{11} + U_{22} + U_{33})/3$.

Table 3. *Selected interatomic distances* (Å)

Ti(1)–O(1)	2.19 (3)	Ti(2)–O(2)	2.06 (2)
Ti(1)–O(1^i)	2.01 (3)	Ti(2)–O(3)	1.76 (3)
Ti(1)–O(2)	1.87 (2)	Ti(2)–O(5)	1.996 (3) ×2
Ti(1)–O(4)	1.997 (3) ×2	Ti(2)–O(6^{ii})	2.29 (3)
Ti(1)–O(6)	1.76 (3)	Ti(2)–O(7)	1.91 (2)
La(1)–O(1)	2.99 (2) ×2	La(2)–O(3)	2.53 (2) ×2
La(1)–O(1^v)	2.62 (2) ×2	La(2)–O(3^{iii})	2.74 (2)
La(1)–O(2)	2.50 (1) ×2	La(2)–O(5^{iv})	2.86 (3)
La(1)–O(4)	2.78 (4)	La(2)–O(7^{iii})	2.53 (2)
La(1)–O(4^{ii})	2.83 (4)	La(2)–O(7^{iv})	2.43 (1) ×2
La(1)–O(4^v)	2.67 (2)		
La(1)–O(5)	2.57 (2)		
La(1)–O(6^{ii})	2.95 (2) ×2		

Symmetry code

None	x,	y,	z		(iii)	$\frac{1}{2} - x$,	$\frac{1}{2} - y$,	$z - \frac{1}{2}$
(i)	x,	$1 - y$,	$z - \frac{1}{2}$		(iv)	x,	y,	$z - 1$
(ii)	x,	y,	$z + 1$		(v)	x,	$1 - y$,	$z + \frac{1}{2}$

parameters are given in Table 2.* Selected interatomic distances are given in Table 3.

Discussion

The crystal structure of $La_2Ti_2O_7$ at 1173 K is shown in Fig. 1. All atoms are on the mirror planes at $x = 0$ and 0.5. The perovskite-type slab contains TiO_6 octahedra and La(1) atoms which are surrounded by twelve O atoms. Neighbouring slabs are joined by the La(2) atoms located at the boundary of the slab. The interatomic distances range from 1.76 (3) to 2.19 (3) Å for Ti(1)–O, from 1.76 (3) to 2.29 (3) Å for Ti(2)–O and from 2.50 (1) to 2.99 (2) Å for La(1)–O. The La(2) atom has five neighbouring O atoms in the same slab and two in the adjacent slab at distances ranging from 2.43 (1) to 2.86 (3) Å. The positional parameters approximately coincide with those for $Sr_2Nb_2O_7$ determined at room temperature (Ishizawa *et al.*, 1975) after taking their origins at an appropriate position on the twofold screw axis. The thermal parameters for $La_2Ti_2O_7$ at 1173 K are twice to three times larger than those for $Sr_2Nb_2O_7$ at room temperature. The structural difference between the $Cmc2_1$ and the $P2_1$ modifications in $La_2Ti_2O_7$ viewed along the b axis is illustrated in Fig. 2. The displacements of the constituent atoms after the phase transition from the $Cmc2_1$ to the $P2_1$ modification are given in Table 4; these are calculated from the values of the cell dimensions at 1173 K and the positional parameters at room temperature (Gasperin, 1975) and those at 1173 K, by shifting the origin of the former structure along the c axis to yield the same z parameter for the La(1) atom as that in the latter structure. The structural change is summarized as: (1) the La atoms move only within the planes $x = 0$ and $x = 0.5$, (2) the O atoms move in such a way that the TiO_6 octahedra rotate around axes parallel to b and running through the respective Ti atoms, and (3) displacements of the Ti atoms are negligible. At room temperature, the TiO_6 octahedra are rotated by approximately 10° from the orientation in the $Cmc2_1$ modification. The magnitudes of the displacements of the La and O atoms are approximately 0.3 Å on average. The displacements of the La atoms are well accommodated to the rotation of the TiO_6 octahedra. These characteristics are quite different from those previously reported for the ferroelectric phase transition between the orthorhombic $Cmcm$ and $Cmc2_1$ modifications of $Sr_2(Ta,Nb)_2O_7$ (Ishizawa *et al.*, 1981). In the ferroelectric phase transition, the B atoms move on the

planes at $x = 0$ and 0.5, destroying the mirror planes perpendicular to the c axis and accompanying a deformation and slight rotation of the BO_6 octahedra around axes parallel to **a**. In the $Cmc2_1$ modification, the spontaneous polarization appears along the c axis chiefly due to the asymmetric deformation of BO_6 octahedra. On the other hand, the $Cmc2_1$–$P2_1$ transition of $La_2Ti_2O_7$ scarcely changes the magnitude of the dipole moment in respective BO_6 octahedra, since the rotation occurs around axes passing through the B cations without deforming the shapes of the octahedra.

There are two kinds of mirror planes in the perovskite slab of the $Cmc2_1$ modification. Owing to the shifts of the constituent atoms on the phase transition from the $Cmc2_1$ modification, the mirror planes on which the Ti atoms lie are lost and those on which the La atoms lie are retained in a slab of the $P2_1$ modification. The surviving mirror planes act as local symmetry elements in the crystal. This is illustrated in Fig. 3. The symmetry change from $Cmc2_1$ to $P2_1$ in $La_2Ti_2O_7$ is described as follows.
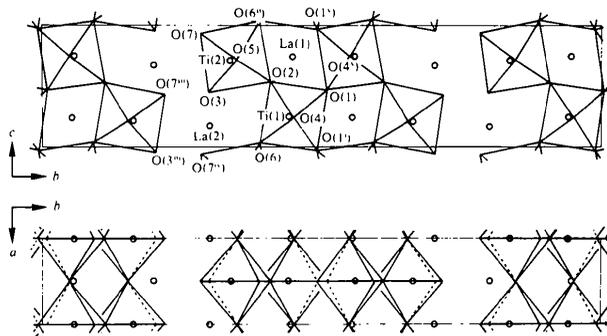

Fig. 1. The structure of the $Cmc2_1$ modification of $La_2Ti_2O_7$ at 1173 K projected along the a (upper) and c (lower) axes.
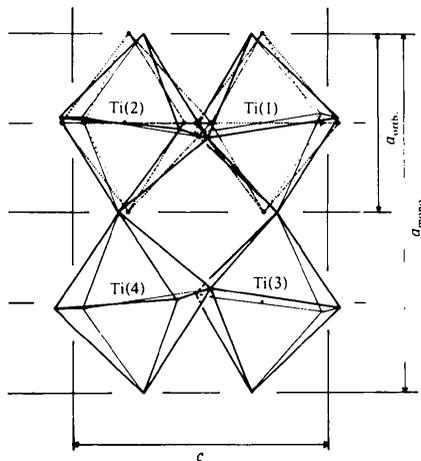

Fig. 2. The linkages of TiO_6 octahedra in the $P2_1$ (solid) and the $Cmc2_1$ (dotted) modifications projected on the (010) plane.

Table 4. Atomic displacement (Å) after the phase transition

x^*	$P2_1$[†]	$Cmc2_1$	δ_x	δ_y	δ_z
0.75	Ti(1)	Ti(1)	−0.02 (1)[‡]	0.00 (1)[‡]	+0.05 (1)[‡]
	Ti(2)	Ti(2)	+0.02 (1)[‡]	+0.04 (1)[‡]	+0.02 (1)[‡]
	O(1)	O(1)	−0.21 (2)	+0.02 (5)[‡]	−0.01 (3)[‡]
	O(2)	O(2)	−0.33 (2)	−0.05 (5)[‡]	+0.06 (3)[‡]
	O(6)	O(6)	+0.11 (2)	−0.03 (5)[‡]	+0.02 (2)[‡]
	O(7)	O(7)	+0.11 (3)	−0.02 (5)[‡]	+0.05 (3)[‡]
	O(3)	O(3)	−0.10 (2)	+0.06 (5)[‡]	+0.06 (2)[‡]
0.5	La(1)	La(1)	0.00 (1)[‡]	−0.08 (1)	0
	La(2)	La(2)	−0.02 (1)[‡]	+0.17 (1)	−0.12 (1)
	O(4)	O(4)	−0.02 (3)[‡]	+0.10 (5)	−0.32 (3)
	O(5)	O(5)	+0.01 (2)[‡]	−0.09 (3)	+0.22 (2)
0.25	Ti(3)	Ti(1)	+0.02 (1)[‡]	−0.01 (1)[‡]	+0.03 (1)[‡]
	Ti(4)	Ti(2)	−0.01 (1)[‡]	0.00 (1)[‡]	+0.04 (1)[‡]
	O(8)	O(1)	+0.21 (2)	−0.03 (5)[‡]	+0.01 (3)[‡]
	O(9)	O(2)	+0.32 (2)	−0.09 (5)[‡]	+0.03 (3)[‡]
	O(13)	O(6)	−0.09 (2)	−0.05 (5)[‡]	−0.01 (2)[‡]
	O(14)	O(7)	−0.11 (2)	+0.13 (5)[‡]	+0.13 (3)[‡]
	O(10)	O(3)	+0.09 (2)	−0.05 (5)[‡]	+0.12 (2)[‡]
0	La(3)	La(1)	−0.01 (1)[‡]	+0.11 (1)	+0.02 (1)
	La(4)	La(2)	+0.01 (2)[‡]	−0.16 (1)	+0.09 (1)
	O(11)	O(4)	+0.01 (2)[‡]	−0.15 (5)	+0.25 (3)
	O(12)	O(5)	0.00 (2)[‡]	+0.07 (5)	−0.35 (2)

* Approximate heights referred to the doubled a axis of the $Cmc2_1$ modification.

† The labels of the atoms are different from those given by Gasperin (1975) but identical to those given for the $P2_1$ modification of $Ca_2Nb_2O_7$ (Ishizawa et al., 1980).

‡ Values should be 0 if the structural change occurs schematically as is illustrated in Fig. 4.
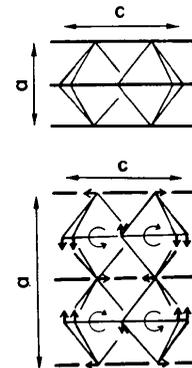

Fig. 3. A schematic drawing of the structural change from the $Cmc2_1$ (upper) to the $P2_1$ (lower) modification.

(1) The a length becomes doubled, making the unit-cell volume of the $P2_1$ modification twice that of the primitive cell of the $Cmc2_1$ modification.

(2) Half of the twofold screw axes in the $Cmc2_1$ modification are lost.

(3) Half of the mirror planes in the $Cmc2_1$ modification are lost and the remainder survive as local symmetry elements which retain their efficiency only within a slab.

(4) The c glide planes of the $Cmc2_1$ modification can be regarded as the secondary symmetry elements generated from the mirror planes and twofold screw axes. Correspondingly, the local n glide planes in the $P2_1$ modification are generated from the local mirror planes and the twofold screw axes.

The symmetry elements of the $Cmc2_1$ and $P2_1$ modifications are illustrated in Fig. 4. The existence of local symmetries is known to provide partial enhancement of the diffraction symmetry (Iwasaki, 1972). The partial orthorhombic symmetry found in hkl reflexions with h even of the $P2_1$ modification originates in the local mirror planes perpendicular to the a axis in each slab.
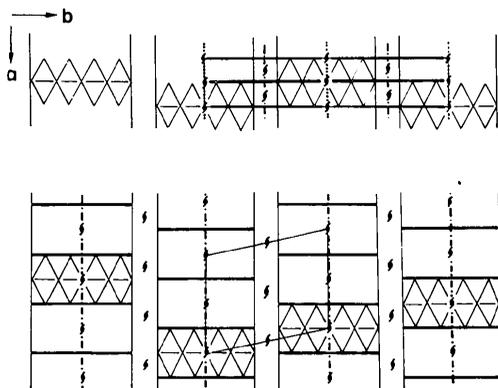

Fig. 4. The symmetry elements of the $Cmc2_1$ (upper) and the $P2_1$ (lower) modifications. The mirror and the n glide planes in the $P2_1$ modification are local symmetry elements effective only within a slab.

Computations were carried out on HITAC M180 and M200H computers at the Computer Center of Tokyo Institute of Technology.

References

COPPENS, P. & HAMILTON, W. C. (1970). *Acta Cryst.* A26, 71–83.
GASPERIN, P. M. (1975). *Acta Cryst.* B31, 2129–2130.
International Tables for X-ray Crystallography (1974). Vol. IV. Birmingham: Kynoch Press.
ISHIZAWA, N., MARUMO, F. & IWAI, S. (1981). *Acta Cryst.* B37, 26–31.
ISHIZAWA, N., MARUMO, F., IWAI, S. KIMURA, M. & KAWAMURA, T. (1980). *Acta Cryst.* B36, 763–766.
ISHIZAWA, N., MARUMO, F., KAWAMURA, T. & KIMURA, M. (1975). *Acta Cryst.* B31, 1912–1915.
ISHIZAWA, N., MARUMO, F., KAWAMURA, T. & KIMURA, M. (1976). *Acta Cryst.* B32, 2564–2566.
ISHIZAWA, N., MIYATA, T., MINATO, I. & IWAI, S. (1978). Report of the Research Laboratory of Engineering Materials, Tokyo Institute of Technology. Vol. 3, pp. 15–18.
IWAI, S., TAGAI, H., KATO, M. & SHIMAMUNE, T. (1971). *Bull. Tokyo Inst. Technol.* 103, 105–109.
IWASAKI, H. (1972). *Acta Cryst.* A28, 253–260.
KIMURA, M. (1977). Private communication.
NANAMATSU, S., KIMURA, M., DOI, K., MATSUSHITA, S. & YAMADA, N. (1974). *Ferroelectrics*, 8, 511–513.
SCHEUNEMANN, K. & MÜLLER-BUSCHBAUM, H. (1974). *J. Inorg. Nucl. Chem.* 36, 1965–1970.
SCHEUNEMANN, K. & MÜLLER-BUSCHBAUM, H. (1975). *J. Inorg. Nucl. Chem.* 37, 1879–1881.

Structure du Polytype Rhomboédrique 3R du Sulfure Double de Fer et de Gallium Fe₂Ga₂S₅

PAR LEILA DOGGUY-SMIRI ET NGUYEN-HUY-DUNG

Laboratoire de Physique (Laboratoire de Chimie Minérale Structurale associé au CNRS n° 200), Faculté des Sciences Pharmaceutiques et Biologiques de Paris V, 4 avenue de l'Observatoire, 75270 Paris CEDEX 06, France

Abstract

The crystal structure of a fifteen S-atom plane polytype of $3R$ Fe₂Ga₂S₅ [$a = 3.6508$ (7), $c = 44.843$ (2) Å, $Z = 3$, space group $R\bar{3}m$, $d_m = 3.85$, $d_x = 3.95$ Mg m⁻³, $\mu = 13.64$ mm⁻¹ (Mo $K\alpha$)] was refined by the least-squares method to a final $R = 0.048$ for 324 reflexions. This structure is built up of a double layer of FeS₆ octahedra enclosed between two single layers of GaS₄ tetrahedra.

The fifth plane of S atoms has metal vacancies. A comparison with other $MM_2'X_5$ (M,M' = metal; X = non-metal, S,Se) and $MM_2'X_4$ structures is made.

Introduction

L'étude du diagramme de phases du système Ga₂S₃–FeS nous a permis d'identifier huit phases inter-